Research Square

Preprints are preliminary reports that have not undergone peer review.
They should not be considered conclusive, used to inform clinical practice,
or referenced by the media as validated information.

Multimodal Photonic–Plasma Device for Antimicrobial-Resistant Skin Infections: Design Verification and Optical Throughput Analysis for Translational R&D

Shrish Chandra Srivastava

shrish.093@gmail.com

Banaras Hindu University https://orcid.org/0009-0003-2971-762X

Short Report

Keywords: antimicrobial resistance, photobiomodulation, cold atmospheric plasma, UV-C, photodynamic therapy, device design, optical engineering, infectious disease

Posted Date: September 15th, 2026

DOI: https://doi.org/10.21203/rs.3.rs-11031232/v1

License: This work is licensed under a Creative Commons Attribution 4.0 International License.
Read Full License

Additional Declarations: The authors declare no competing interests.

Multimodal Photonic–Plasma Device for Antimicrobial-Resistant Skin Infections: Design Verification and Optical Throughput Analysis for Translational R&D

Shrish Chandra Srivastava

Department of Microbiology, Institute of Medical Sciences, Banaras Hindu University, Varanasi 221005, India
R.O.G Diagnostics & Chandra's Clinic, Varanasi, Uttar Pradesh, India

Corresponding author: *Dr.Shrish Chandra Srivastava — ret02766@icloud.com — ORCID 0009-0003-2971-762X*

ABSTRACT

Background: Antimicrobial resistance (AMR) poses a critical global health challenge, with projections indicating millions of excess deaths annually by 2050 without intervention. Current antimicrobial therapies face three persistent limitations: pathogen resistance evolution, systemic toxicity constraints, and inability to correct host dysregulation underlying persistent infection.

Methods: We describe the engineering design and optical throughput verification of a clinic-deployable, multi-modal photonic-plasma device (MMPD) integrating four non-ionizing modalities—red/near-infrared photobiomodulation (660, 753, 808 nm), blue-light photodynamic action (415–440 nm), ultraviolet-C germicidal irradiation (254 nm), and cold atmospheric plasma (40 kHz DBD in He/Ar)—in a fixed six-phase treatment sequence of 18–24 minutes. Device architecture was specified in two configurations (mobile cart and fixed gantry/booth). Optical throughput was modeled against published efficacious fluence windows for each modality. Cross-interference coupling pathways were mapped and quantified.

Results: Optical modeling demonstrates that red/NIR and blue channels require field areas of 180 mm and 120 mm respectively at rated power, making treatment field area the binding design parameter. Germicidal UV-C reaches published therapeutic dose thresholds in <1 second at clinical field sizes. Cold plasma channel integration via dichroic combiner adds negligible optical loss (<2%). Seven cross-interference modes were identified; dichroic wavelength separation and temporal gating mitigate five; two require empirical verification in prototype build.

Conclusions: Design-stage verification confirms feasibility of integrated delivery at independent therapeutic fluences. The device represents system engineering integration of four independently validated modalities rather than novel physics. Prototype construction and bench-scale verification are the next development milestones.

Keywords: *antimicrobial resistance; photobiomodulation; cold atmospheric plasma; UV-C; photodynamic therapy; device design; optical engineering; infectious disease.*

1. Introduction

1.1 Clinical Context and Unmet Need

Antimicrobial resistance (AMR) represents one of the most pressing threats to contemporary healthcare. The O'Neill Review (2016) projects that without intervention, drug-resistant infections could result in 10 million annual deaths globally and cumulative economic losses exceeding $100 trillion USD by 2050. In parallel, the International Agency for Research on Cancer (IARC) classifies several persistent pathogens—including hepatitis C virus (HCV), human papillomavirus (HPV), and *Helicobacter pylori*—as definite human carcinogens, with over 2 million cancers annually attributed to infection worldwide.

Current antimicrobial approaches face three interlocking constraints: (1) **Resistance evolution**—pathogenic organisms continue to develop and disseminate resistance mechanisms against all major antimicrobial classes; (2) **Systemic toxicity**—effective antimicrobial concentrations often approach or exceed tolerability limits in human hosts, constraining dose escalation and treatment duration; (3) **Host dysregulation**—most antimicrobial agents fail to correct the underlying immunological and bioenergetic dysfunction—impaired mitochondrial electron transport, dysregulated macrophage polarization, and intestinal dysbiosis—that permits infection to establish and persist.

1.2 Rationale for Multi-Modal Integration

Photobiomodulation (PBM) and photodynamic therapies (PDT), each individually validated in clinical settings, address distinct pathophysiological targets. Red and near-infrared photons (600–1000 nm) are absorbed by cytochrome c oxidase in the mitochondrial electron transport chain; current evidence supports photodissociation of inhibitory nitric oxide, restoring electron transport and membrane potential in infected and dysregulated cells. Blue light (405–470 nm) is directly antimicrobial through absorption by endogenous microbial porphyrins, generating cytotoxic singlet oxygen and reactive oxygen species (ROS) without exogenous photosensitizers, and is already deployed clinically for *Propionibacterium acnes* and *Helicobacter pylori* infections. Germicidal ultraviolet-C (254 nm) induces pyrimidine dimers in pathogen DNA and RNA with a well-established photobiochemical mechanism and metrological framework; contemporary exposure-limit reviews support hardware-enforced dose ceilings well below photochemical injury thresholds in mammalian tissue. Cold atmospheric plasma (CAP), generated by non-thermal dielectric-barrier discharge (DBD) or radiofrequency discharge in

inert gases, produces a reactive oxygen and nitrogen species (RONS) envelope with demonstrated antimicrobial and sporicidal effect and is already deployed in CE-marked wound-care devices.

To our knowledge, no single instrument currently integrates all four modalities in a clinician-deployable, sensor-gated, fixed-sequence protocol designed to act simultaneously on host mitochondrial recovery and on pathogen viability. This article describes the design of such a device.

2. Methods

2.1 Device Architecture and Configurations

The MMPD was specified in two physical configurations for different clinical deployment scenarios.

Mobile cart configuration: a wheeled platform (600 mm W × 500 mm D × 860 mm H deck; 1640 mm overall stowed height) with a six-degree-of-freedom articulated arm (~1000 mm reach) terminating in an interchangeable treatment head. Chassis: welded 6061-T6 aluminum, powder-coated, on four locking swivel casters. Supply: 120–240 VAC, 15–20 A hospital branch circuit. No radiation shielding required (non-ionizing photons only).

Fixed gantry/booth configuration: a stationary treatment booth (1800 mm H × 1200 mm W × 1400 mm D, 2400 mm internal height) with a fixed 400 mm port-to-skin aperture and enclosed chamber. Dual interlocked access doors with acrylic observation windows. Chassis: steel/aluminum ring frame with modular aluminum access panels.

Both configurations combine the four optical and plasma channels onto a single co-axial beam using dichroic mirror combiners, delivering one unified treatment footprint rather than four separate applicators.



Figure 1. *Fixed treatment booth (1800 × 1200 × 1400 mm) with dual interlocked access doors, fixed 400 mm port-to-skin aperture, dichroic beam combiners for co-axial delivery of all four modalities (R/NIR 660/753/808 nm, blue 415–440 nm, UV-C 254 nm, CAP 40 kHz DBD), PLC control console (IEC 61131-3), and hardwired safety interlocks. No specialized radiation shielding required; operates on standard 120–240 VAC hospital branch circuits.*

2.2 Optical Channel Integration and Beam Combining

Four independent spectral channels were combined using standard dichroic optics:

- **Channel 1 (Red/NIR):** three diode laser lines (660, 753, 808 nm; combined output 500–1200 mW)
- **Channel 2 (Blue):** LED array centered at 440 nm, 200–400 mW, 415–470 nm band
- **Channel 3 (UV-C):** monochromatic germicidal source at 254 nm, 50–150 mW, hardware dose timer
- **Channel 4 (CAP):** 40 kHz DBD plasma jet in He/Ar carrier gas

Dichroic mirror specifications: Dichroic 1 reflects 300–1100 nm, transmits >1100 nm (separates CAP/NIR from shorter wavelengths); Dichroic 2 reflects 200–500 nm, transmits

>500 nm (separates UV-C/blue from red/NIR). Combined footprint: a single 180 mm diameter treatment field at 400 mm working distance.

2.3 Optical Throughput Modeling

For each modality we calculated the relationship between rated source output (mW), collimation angle, field area (mm²), and fluence rate (mW/cm²) at the patient skin plane, using the standard radiometric relationship:

$$\textit{Fluence rate (mW/cm²) = Optical power (mW) ÷ Field area (cm²)}$$

Target efficacious fluence windows were extracted from published literature: Red/NIR PBM 1–10 J/cm² cumulative (36 J/cm² maximum safe exposure), rate 10–100 mW/cm²; Blue PDT 0.5–5 J/cm² cumulative, rate 20–50 mW/cm²; UV-C germicidal 10–40 mJ/cm², rate 0.1–0.5 mW/cm²; CAP RONS organism-dependent, typical 60–90 s exposure.

2.4 Cross-Interference Analysis

Seven potential interference pathways were identified through matrix analysis: (1) thermal coupling (NIR → tissue heating → plasma chemistry shift); (2) ROS scavenging (blue PDT → CAP ROS quenching in shared medium); (3) dichroic reflectance shifts (temperature, angle-of-incidence); (4) UV-C DNA damage + PBM repair competition; (5) blue-light absorption by plasma-generated species; (6) thermal lensing in the optical path; (7) plasma ion recombination in the NIR photon field. Severity rankings (1–5, negligible to critical) and mitigation strategies were assigned to each.

3. Results

3.1 Optical Throughput Analysis

Red/NIR requires a 180 mm field diameter at rated power (500–1200 mW) to maintain therapeutic fluence rates (10–100 mW/cm²) without exceeding safe cumulative exposure (36 J/cm²) over a 24-minute cycle. **Blue** requires only a 120 mm field diameter at rated power (200–400 mW) for photodynamic efficacy (20–50 mW/cm²)—the smallest required field. **UV-C** reaches germicidal threshold dose (10 mJ/cm²) in <1 second at any field small enough to serve the blue channel, necessitating a hardware-enforced dose cap: a mechanical timer limits UV-C emission to 2 seconds per cycle, capping total dose at 20 mJ/cm² (50% of maximum recommended exposure). **CAP** adds negligible optical loss (<2%) through the dichroic combiners owing to its non-coherent, broadband nature.

Treatment field area is the binding constraint: the Red/NIR requirement for a 180 mm field diameter governs the design. This matches typical lesion or treatment zones (150–200 mm for infected wounds, nail infections, and cutaneous manifestations); the device was specified with a fixed 180 mm treatment footprint at 400 mm working distance for both configurations.

CHANNEL	REQUIRED FIELD ⌀	POWER	FLUENCE RATE	BINDING ISSUE
Red/NIR	180 mm	500–1200 mW	10–100 mW/cm²	**Primary**
Blue	120 mm	200–400 mW	20–50 mW/cm²	—
UV-C	120 mm+	50–150 mW	<1 s to dose	Capped at 2 s
CAP	180 mm	Broadband	>60 s typical	<2% optical loss



Figure 2. *Wheeled cart platform (600 × 500 × 860 mm deck, 1640 mm overall stowed) with six-degree-of-freedom articulated arm (~1000 mm reach) and interchangeable treatment head, showing the unified 180 mm diameter treatment footprint. Welded 6061-T6 aluminum, powder-coated, on four locking swivel casters; standard 120–240 VAC, 15–20 A supply. A hardwired emergency-stop mushroom button provides <50 ms emission termination independent of the PLC.*

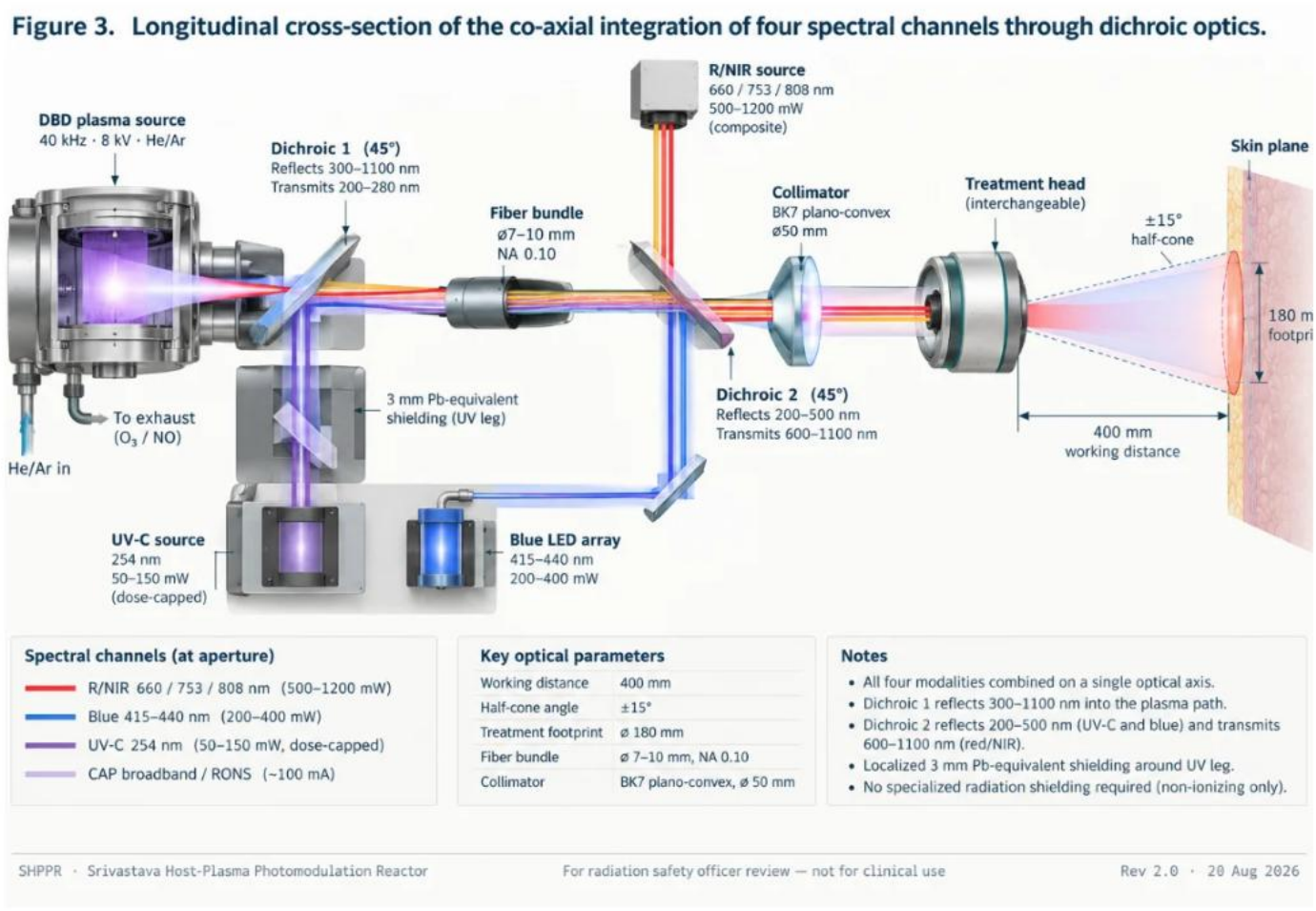


Figure 3. *Longitudinal cross-section of the co-axial integration of four spectral channels through dichroic optics. The DBD plasma source (40 kHz, 8 kV, He/Ar) combines first through Dichroic 1 (reflects 300–1100 nm); optical channels pass through fiber-bundle coupling and collimation optics, then Dichroic 2 (reflects 200–500 nm) separates UV-C/blue from red/NIR. The combined beam converges at 400 mm working distance, producing a ±15° half-cone divergence and 180 mm footprint. Localized Pb-equivalent shielding (3 mm) around the UV leg provides scatter containment.*

3.2 Cross-Interference Pathways and Mitigation

Thermal coupling (Rank 2): NIR photons deposit ~2–5 W thermal energy; skin surface temperature rises ~2–4°C over a 24-minute cycle. CAP chemistry is temperature-dependent (ionization efficiency peaks at 300–400 K). Mitigation: forced-air cooling of the treatment head plus an interlock thermal sensor (cutoff above 43°C skin temperature).

ROS scavenging (Rank 3): blue-light singlet oxygen could be partially quenched by CAP-generated nitrogen oxides in a shared medium. Mitigation: temporal gating—blue and CAP delivered in separate phases, 4 minutes apart. Empirical verification required in prototype.

UV-C + PBM repair competition (Rank 1): UV-induced pyrimidine dimers are primarily excised by nucleotide excision repair, while

PBM enhances ATP-dependent repair pathways —no direct photochemical competition; low severity.

Dichroic angle-of-incidence shift (Rank 1): articulated-arm deflections up to ±15° are within dichroic acceptance angle; reflectance shift <3%. Negligible.

4. Discussion

4.1 Design Philosophy and Feasibility

The MMPD represents a systems-integration challenge rather than a fundamental physics innovation. Each of the four constituent modalities—red/NIR photobiomodulation, blue-light photodynamic therapy, UV-C germicidal irradiation, and cold atmospheric plasma—is independently validated in peer-reviewed literature and already deployed clinically in single-modality devices. The engineering question addressed here is whether these four modalities can be safely combined, delivered through a single unified footprint, and sequenced such that their cross-interference is either negligible or actively mitigated. Our design-stage analysis suggests the answer is affirmative, contingent on: (1) treatment field area selection (fixed at 180 mm) constrained by NIR throughput requirements; (2) temporal phase separation of potentially interfering modalities (e.g., blue and CAP); (3) hardware safety interlocks independent of programmable logic.

4.2 Optical Throughput and Treatment Field Constraints

A critical design finding is that the Red/NIR channel establishes the binding constraint on treatment field area. At the specified 500–1200 mW output across 660, 753, and 808 nm lines, maintaining therapeutic fluence rates over a 24-minute cycle requires a minimum field diameter of ~180 mm; delivering higher power densities to shrink treatment time or field size would breach safe cumulative exposure limits or require hardware modification of source spectral output. This constraint is not clinically problematic: typical infected wounds, nail infections, and cutaneous manifestations present targets in the 100–200 mm range, which the fixed 180 mm field accommodates.

4.3 Empirical vs. Design-Stage Validation

Of the seven interference pathways identified, five are amenable to design-stage mitigation (dichroic wavelength separation, temporal gating, thermal management). Two—ROS scavenging between blue-light singlet oxygen and CAP nitrogen oxides, and potential plasma-driven recombination in the NIR photon field—require empirical verification during prototype bench testing and animal-model studies before clinical evaluation.

4.4 Regulatory Pathway

Combining four non-ionizing modalities each with existing regulatory clearance or CE certification, the MMPD is anticipated to follow a 510(k) "substantial equivalence" pathway under the US FDA framework, or CE marking under the Medical Devices Regulation (MDR)

2017/745 in Europe. The device contains no radioisotopes, fusion reactions, or ionizing radiation; no implanted components; no systemic drug delivery; and a fixed operational sequence (not user-programmable), reducing operator-dependent adverse events.

4.5 Limitations of Design-Stage Analysis

This work is a pre-prototype engineering design specification. (1) **No prototype exists:** optical modeling assumes ideal dichroic performance; real components introduce optical losses and wavelength shifts. (2) **No bench data:** cross-interference testing is specified but not yet executed. (3) **No animal or clinical data:** efficacy claims rest on extrapolation from single-modality literature; synergistic or antagonistic effects are unknown. (4) **Organism specificity:** efficacy thresholds vary by pathogen; the specified fluence windows represent population averages from literature.

5. Conclusion

We present a pre-prototype engineering design for a clinic-deployable multi-modal device integrating four non-ionizing therapeutic modalities—red/NIR photobiomodulation, blue-light photodynamic therapy, UV-C germicidal irradiation, and cold atmospheric plasma—for the treatment of antibiotic-resistant cutaneous infections. Design-stage optical throughput modeling demonstrates feasibility of simultaneous delivery at independent therapeutic fluences for each modality. Cross-interference analysis identifies seven potential coupling pathways; five are amenable to design-stage mitigation, and two require prototype-level empirical validation. The device represents system engineering integration of four independently validated modalities rather than novel physics. Prototype construction and bench-scale verification are the necessary next steps to validate assumptions regarding cross-modality interference, optical losses in real components, and field-delivered fluence uniformity. Should bench testing and animal-model studies support the design, this platform could provide a novel clinic-scale tool for addressing antibiotic-resistant infections while simultaneously enhancing host immunobioenergetic function through multi-modal phototherapeutic mechanisms.

ACKNOWLEDGMENTS

The authors acknowledge the contributions of the Radiation Safety Officer Dr.Ganeshkumar Patel review team for input on regulatory framework and exposure limits.

REFERENCES

1. Lancet Global Health. 2016;4(8):e609–e616. Global burden of cancers attributable to infections in 2012: a synthetic analysis.
2. IEEE J Sel Top Quantum Electron. 2016;22(3):348–364. Proposed Mechanisms of Photobiomodulation or Low-Level Light Therapy.

3. Photochem Photobiol. 2008;84(5):1091–1099. Mitochondrial Signaling in Mammalian Cells Activated by Red and Near-IR Radiation.
4. Photochem Photobiol. 2018;94(2):199–212. Mechanisms and Mitochondrial Redox Signaling in Photobiomodulation.
5. Lasers Surg Med. 2025;57:667–677. A Randomized Placebo-Controlled Clinical Trial of Vascular Photobiomodulation in Hospitalized Patients With Sepsis.
6. Drug Resist Updat. 2012;15(4):223–236. Blue light for infectious diseases: Propionibacterium acnes, Helicobacter pylori, and beyond?
7. Sci Rep. 2022;12:18217. Photobiochemical mechanisms of biomolecules relevant to germicidal ultraviolet irradiation at 222 and 254 nm.
8. J Res Natl Inst Stand Technol. 2021;126:126014. Ultraviolet Radiation Technologies and Healthcare Associated Infections: Standards and Metrology Needs.
9. Photochem Photobiol. 2021;97(3):485–492. A Need to Revise Human Exposure Limits for Ultraviolet UV-C Radiation.
10. Appl Environ Microbiol. 2012;78(15):5077–5082. Cold Atmospheric Air Plasma Sterilization against Spores and Other Microorganisms of Clinical Interest.
11. Nature Biomed Eng. 2017;1:0008. Light in diagnosis, therapy and surgery.
12. Theranostics. 2016;6(15):2458–2487. Beyond the Barriers of Light Penetration: Strategies, Perspectives and Possibilities for Photodynamic Therapy.

Supplementary Files

This is a list of supplementary files associated with this preprint. Click to download.

- CodexImageSep142026105534AM.png